Electronic Materials Letters, Vol. 5, No. 3 (2009), pp. 135-138
DOI: 0.3365/eml.2009.09.135

Growth of ZnO Nanorods on Various Substrates by Electrodeposition

Hyunghoon Kim, Jin Young Moon, and Ho Seong Lee*

School of Materials Science and Engineering, Kyungpook National University,
1370 Sangyeok-dong, Buk-gu, Daegu 702-701, Korea

The structural and optical properties of electrochemically grown ZnO nanorods on several substrates were investigated. The ZnO nanorods were dense and vertically well-aligned with the decrease in resistivity of substrates. Scanning and transmission electron microscopy results showed that hexagon-shaped ZnO nanorods with a diameter in the range of 100 nm to 200 nm and a length of about 600 nm were formed. Photoluminescence (PL) measurement showed a strong near-bandedge UV emission at 382 nm and a broader band emission centered around 600 nm, which was related to deep level defects.

Keywords: ZnO, Nanorods, Electrodepositon

1. INTRODUCTION

Zinc oxide (ZnO) has attracted global interest for potential applications, such as electronic and optoelectronic devices, solar cells, and chemical sensors, because of its direct wide bandgap of 3.37 eV and large exciton binding energy of 60 meV.[1,2] Recently, nano ZnO transistors,[3] nano ZnO light emitting diodes (LEDs),[4] nanorod laser devices,[5] and dye-sensitized solar cells (DSSC)[6] have been reported.

So far, for the realization of these ZnO-based nano-devices, ZnO has been prepared by many different techniques, such as plasma enhanced molecular beam epitaxy (PEMBE),[7] thermal chemical vapor deposition (CVD),[8] sol-gel,[9] and vapor-liquid-solid (VLS)[10,11] growth. However, there are some problems concerning the control of the dimensionality and doping. For example, in the VLS growth method, the control of the dimensionality of nanowires depends on the eutectic temperature and size of the liquid droplet. Nanowires, which have large size distribution, grow on the liquid droplet.

Electrodeposition, as another approach method, has several advantages compared with the deposition technologies mentioned above.[12-14] Electrochemical deposition is a low cost and low temperature process. The dimensionality can be easily controlled by varying the concentration of solution and applied potential. ZnO films were electrodeposited on several substrates such as GaN,[15] Au,[16] indium tin oxide (ITO),[17] and Zn plate.[18] The electrochemical approaches were performed by several groups.[15-19] Typically, ZnO were cathodically electrodeposited in oxygen-saturated aqueous salt solution below 100℃. The growth mode can change from two dimensional films to three dimensional nanorods by varying growth conditions.[19,20] There are several factors that affect the microstructure of ZnO films: the lattice constant of a substrate, the electrolyte, the dissolved oxygen content, the cell potential, and the pretreatment of the electrode surface. The core-shell nanostructures can tune the electrical and optical properties of ZnO nanorods.[21-23]

In this study, we report the growth of vertically well-aligned ZnO nanorods by cathodic electrodeposition in aqueous zinc chloride electrolyte. The effect of the substrate on the growth of ZnO nanorods by electrodeposition was investigated. The microstructural and optical properties of ZnO nanorods were characterized.

2. EXPERIMENTAL PROCEDURE

ZnO nanorod arrays were electrodeposited in electrolyte solutions composed of 5 mM $ZnCl_2$ and 0.1 M KCl. The substrates used were Au/Si, amorphous Zn-doped In_2O_3 (a-IZO), In-doped ZnO/Si, and bare Si (001). The resistivities of the substrates were 4.2×10^{-6}, 2.8×10^{-4}, and 2.5×10^{-4} Ωcm, respectively. The resistivity of a bare Si substrate could not be measured. Prior to the electrodeposition, the substrates were ultrasonically cleaned with acetone, ethanol, and de-ionized water for 5 min, respectively. The electrodepositon was performed in a two-electrode electrochemical cell at 80℃. The above-mentioned substrates and gold-coated Si were used as a working and a counter electrode, respectively. The potential applied to the working electrode was -1.0 V. The deposition time was 30 min. During the electrodeposition, oxygen gas was continuously bubbled near the working electrode. The dissolved oxygen functions as an oxygen

*Corresponding author: hs.lee@knu.ac.kr

source necessary to ZnO nanorod growth. The deposition reaction in the electrolyte is as follows:[24]

$$Zn^{2+} + 1/2O_2 + 2e^- \rightarrow ZnO$$

This occurs if the negative potential is applied to the working electrode. The apparatus used in this study was shown schematically in Fig. 1. After electrodepositing, the samples were annealed at 130°C for 15 min in air to remove the remaining water.

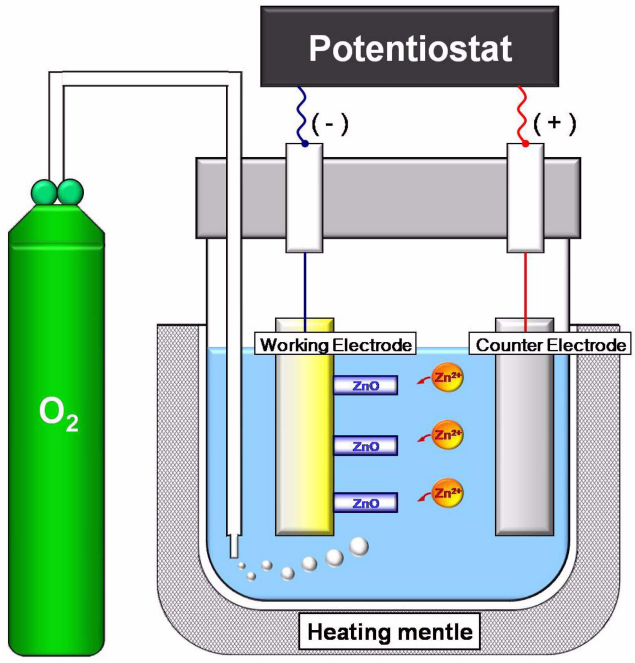

Fig. 1. Schematic diagram of the apparatus used in the electrodeposition of ZnO nanorods.

The morphology of the product was analyzed by field emission scanning electron microscopy (FESEM). The crystal structure and crystallinity of the prepared ZnO nanostructures were characterized by x-ray diffraction (XRD) and transmission electron microscopy (TEM). For the characterization of optical properties, some samples were annealed at 300°C for 1 h in air. Photoluminescence (PL) measurement was carried out at room temperature under excitation with a 30 mW He-Cd laser operating at 325 nm.

3. RESULTS AND DISCUSSION

Figure 2 is FESEM images of the ZnO nanorod arrays grown on several substrates for 30 min. ZnO nanorod arrays grown on Au/Si substrates are vertically well-aligned and very dense, as shown in Fig. 2(a). The substrate is covered by the ZnO nanorods, which has a diameter in the range of 100 nm to 200 nm. The inset of Fig. 2(a) is a high-magnified FESEM image of a single ZnO nanorod, showing a nearly perfect hexagon facet. ZnO nanorods grown on ZnO/Si substrates have vertically random orientation and cover the substrate perfectly, as shown in Fig. 2(b). The diameter of the ZnO nanorods grown on ZnO/Si substrates is slightly larger than that of ones grown on Au/Si substrates. The top surface of a ZnO nanorod is slightly faceted. Figure 2(c) shows randomly oriented ZnO nanorods and large plates grown on an *a*-IZO/Si substrate. Figure 2(d) shows the film grown on a bare Si (001) substrate, showing a few ZnO nanorods. ZnO nanorods are rarely grown on Si substrates because of the

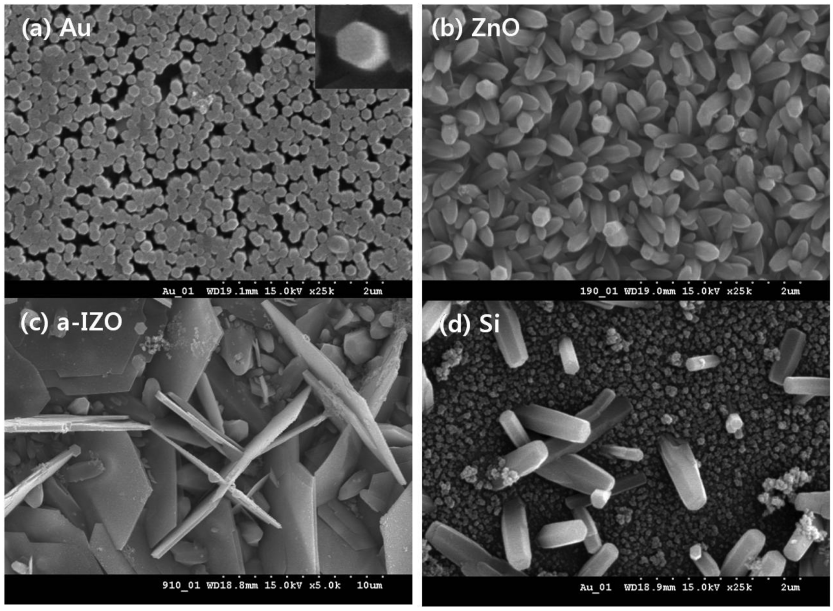

Fig. 2. FESEM images of the ZnO nanorod arrays grown on several substrates for 30 min at 80°C and -1.0 V. (a) Au/Si, (b) ZnO/Si, (C) *a*-IZO/Si, and (d) bare Si substrates.

very low conductivity of the Si substrate. This different morphology is related to the difference in the conductivity of the substrate.

Figure 3 shows the 2θ-ω XRD patterns of ZnO nanorods annealed at 130°C for 15 min in air to remove the remaining water. The diffraction patterns can be indexed to diffraction peaks from ZnO and substrates. The diffraction patterns related to ZnO reveal the hexagonal wurtzite structure (JCPDS No. 36-1451, a = 0.324 nm, c = 0.5206 nm). The diffraction intensity of (0002) planes in Figs. 3(a) and (b) is higher than those of other peaks, indicating that ZnO nanorods have preferred orientation along the [0001] direction. This is also confirmed by TEM analysis. The c-axis is the favorable growth direction because the polar (0002) plane is metastable.[16] ZnO nanorods grown on a-IZO and Si substrates show very weak diffraction intensities and have no preferred orientation, as shown in Figs. 3(c) and (d).

Further microstructural characterization of the ZnO nanorods was carried out by TEM. Figure 4 shows a cross-sectional bright-field TEM micrograph of ZnO nanorods grown on a Au/Si substrate and the corresponding selected area electron diffraction (SAED) pattern. The sample exhibits a columnar structure with a smooth surface and uniform length. The length of ZnO nanorods is about 600 nm. ZnO nanorod arrays are vertically well-aligned. An abrupt interface between the ZnO nanorods and Au/Si substrate is observed. The SAED pattern of a single ZnO nanorod can be indexed to the wurtzite structure of hexagonal ZnO, which confirms that ZnO nanorods are single crystals. The zone axis is [11$\bar{2}$0], indicative of the growth of the ZnO nanorods along the [0001] direction, which is consistent with the XRD result.

Figure 5 is a room temperature PL spectrum of ZnO nanorods grown on a Au/Si substrate after annealing at 300°C for 1 h in air. The PL spectrum reveals a strong ultraviolet band emission at 382 nm and a relatively weak visible band emission centered at 600 nm. The UV PL peak at 382 nm and the

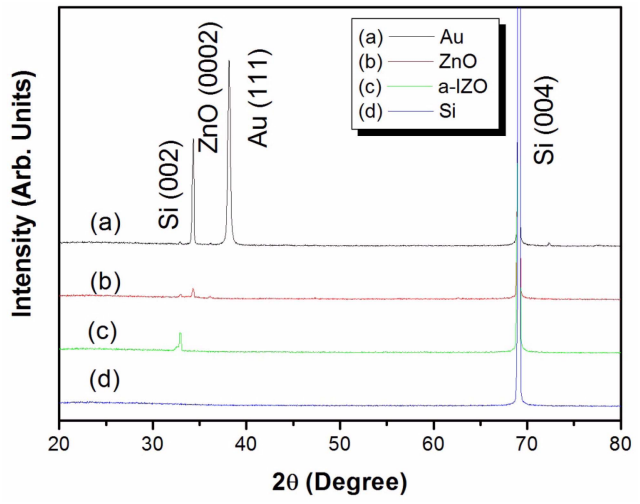

Fig. 3. XRD patterns of the ZnO nanorods annealed at 130°C for 15 min in air. (a) Au/Si, (b) ZnO/Si, (C) a-IZO/Si, and (d) bare Si substrates.

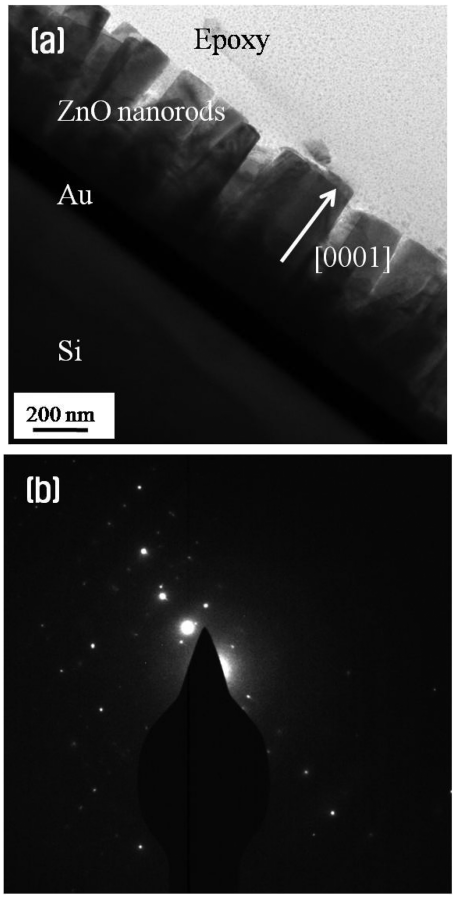

Fig. 4. (a) Cross-sectional bright-field TEM micrograph of ZnO nanorods grown on a Au/Si substrate and (b) the corresponding SAED pattern. ZnO nanorods were vertically well-aligned and grown along the [0001] direction.

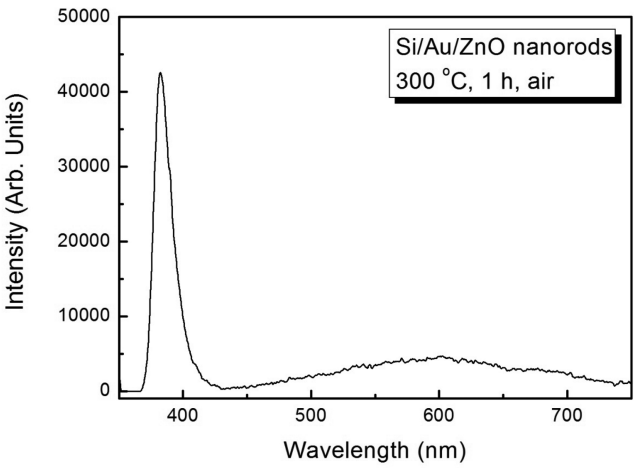

Fig. 5. Room temperature PL spectrum of the ZnO nanorods grown on a Au/Si substrate after annealing at 300°C for 1 h in air.

broad visible emission bands around 600 nm are related to the near band-edge emission and the recombination at the deep defect levels, respectively. The ratio of the intensity of the near band edge emission to the intensity of the deep level emission (I_{NBE}/I_{DLE}) is large, as shown in Fig. 5, indicating a relatively low concentration of deep level defects. The PL result together with the SEM and XRD results indicates the conductivity of the substrate is a very important factor for obtaining the good crystallinity and optical quality of ZnO nanorods grown by electrodeposition

4. SUMMARY

ZnO nanorods were successfully grown by electrodeposition on several substrates at 80°C under the potential of -1.0 V. The conductivity of conductive substrates greatly affects on the structural and optical properties of ZnO nanorods. More conductive substrates favor high quality ZnO nanorod growth. PL measurement showed a near band edge UV emission and a broader band emission related to deep level defects. Low temperature electrodeposition on conductive substrates can be applied in the simple mass production of well-aligned ZnO nanorods.

ACKNOWLEDGEMENT

This work was supported by the Korea Science and Engineering Foundation (KOSEF) grant funded by the South Korean government (MEST) (No. 2009-0068850).

REFERENCES

1. M. Willander, O. Nur, Q. X. Zhao, L. L. Yang, M. Lorenz, B. Q. Cao, J. Zuniga Perez. C. Czekalla, G. Zimmermann, M. Grundmann, A. Bakin, A. Berhrends, M. Al-Suleiman, A. El-Shaer, A. Che Mofor, B. Postels, A. Waag, N. Bookos, A. Travlos, H. S. Kwack, J. Guinard, and D. Le Si Dang, *Nanotechnology* **20**, 332001 (2009).
2. C. H. Ahn, Y. Y. Kim, S. W. Kang, B. H. Kong, S. K. Mohanta, H. K. Cho, J. H. Kim, and H. S. Lee, *J. Mater. Sci.: Mater. Electron.* **19**, 744 (2008).
3. J. Yoo, C. H. Lee, Y. J. Doh, H. S. Jung, and G. C. Yi, *Appl. Phys. Lett.* **94**, 223117 (2009).
4. R. Konenkamp, R. C. Word, and C. Schiegel, *Appl. Phys. Lett.* **85**, 6004 (2004).
5. G. P. Zhu, C. X. Xu, J. Zhu, C. G. Lv, and Y. P. Cui, *Appl. Phys. Lett.* **94**, 051106 (2009).
6. J. H. Noh , S. H. Lee, S. W. Lee, and H. S. Jung, *Electron. Mater. Lett.* **4**, 71 (2008).
7. G. Zhang, A. Nakamura, T. Aoki, J. Temmyo, and Y. Matsui, *Appl. Phys. Lett.* **89**, 113112 (2006).
8. A. J. Cheng, Y. Tzeng, Y. Zhou, M. Park, T. Wu, C. Shannon, D. Wang, and W. Lee, *Appl. Phys. Lett.* **92**, 092113 (2008).
9. K. P. Misra, R. K. Shukla, A. Srivastava, and A. Srivastava, *Appl. Phys. Lett.* **95**, 031901 (2009).
10. B. H. Kong, D. C. Kim, Y. Y. Kim, and H. K. Cho, *J. Korean Phys. Soc.* **49**, S741 (2006).
11. I. Levin, A. Davydov, B. Nikoobakht, N. Sanford, and P. Mogilevsky, *Appl. Phys. Lett.* **87**, 103110 (2005).
12. Q. Wang, G. Wang, J. Jie, X. Han, B. Xu, and J. G. Hou, *Thin Solid Films* **492**, 61 (2005).
13. M. Izaki and T. Omi, *J. Electrochem. Soc.* **143**, L53 (1996).
14. S. Peulon and D. Lincot, *Adv. Mater.* **8**, 166 (1996).
15. T. Pauporte, D. Lincot, B. Viana, and F. Pelle, *Appl. Phys. Lett.* **89**, 233112 (2006).
16. G. W. She, X. H. Zhang, W. S. Shi, X. Fan, J. C. Chang, C. S. Lee, S. T. Lee, and C. H. Liu, *Appl. Phys. Lett.* **92**, 053111 (2008).
17. L. Xu, Q. Liao, J. Zhang, X. Ai, and D. Xu, *J. Phys. Chem.* **C 111**, 4549 (2007).
18. M. H. Wong, A. Berenov, X. Qi, M. J. Kappers, Z. H. Barber, B. Illy, Z. Lockman, M. P. Ryan, and J. L., *Nanotechnology* **14**, 968 (2003).
19. R. E. Marotti, D. N. Guerra, C. Bello, G. Machado, and E. A. Dalchiele, *Sol. Energy Mater. Sol. Cells* **82**, 85 (2004).
20. G. She, X. Zhang, W. Shi, X. Fan, and J. C. Chang, *Electrochem. Commun.* **9**, 2784 (2007).
21. J. Yoo, Y. J. Hong, H. S. Jung, Y. J. Kim, C. H. Lee, J. Cho, Y. J. Doh, L. S. Dang, K. H. Park, and G. C. Yi, *Adv. Funct. Mater.* **19**, 1601 (2009).
22. C. Y. Chen, C. A. Lin, M. J. Chen, G.R. Lin, and J. H. He, *Nanotechnology* **20**, 185605 (2009).
23. N. O. V. Plank, H. J. Snaith, C. Ducati, J. S. Bendall, L. Schmidt-Mende, and M. E. Welland, *Nanotechnology* **19**, 465603 (2008).
24. S. Peulon and D. Lincot, *J. Electrochem. Soc.* **145**, 864 (1998).